

Diffraction anomalies in hybrid structures based on chalcogenide-coated opal photonic crystals

M. M. Voronov,* A. B. Pevtsov, S. A. Yakovlev, D. A. Kurdyukov, and V. G. Golubev
Ioffe Physical-Technical Institute of the Russian Academy of Sciences, St. Petersburg 194021, Russia

The results of spectroscopic studies of the diffraction anomalies (the so-called resonant Wood anomalies) in spatially-periodic hybrid structures based on chalcogenide ($\text{Ge}_2\text{Sb}_2\text{Te}_5$)-coated opal films of various thickness are presented. A theoretical analysis of spectral-angular dependencies of the Wood anomalies has been made by means of a phenomenological approach using the concept of the effective refractive index of waveguiding surface layer.

PACS numbers: 42.25.Fx, 42.70.Gi, 78.66.-w, 78.67.Pt

I. INTRODUCTION

In recent years, investigations of periodic hybrid structures, which are 2D and 3D photonic crystals covered with a thin metal or dielectric film, have attracted an increasing interest.¹⁻⁵ The aim of the present work is to study character of the optical response of hybrid structures consisting of the spatially-ordered opal film coated with a high refractive index material. The chalcogenide compound $\text{Ge}_2\text{Sb}_2\text{Te}_5$ (denoted by GST225) with a refractive index greater than 4 has been chosen to use.⁶ Another reason for the choice is a rather simple technique for fabrication of $\text{Ge}_2\text{Sb}_2\text{Te}_5$ films on the opal surface.⁷ It should be mentioned that Ge-Sb-Te based chalcogenides are used in rewritable optical data storage applications and non-volatile phase change memory devices.^{6,8,9} In Refs. 7 and 10 it is shown that the light reflection spectra from opal/ $\text{Ge}_2\text{Sb}_2\text{Te}_5$ hybrid structures demonstrate the resonant Wood anomalies, caused by the interaction of the incident electromagnetic radiation with the hexagonally arranged surface layer of the hybrid structure. A theoretical study of optical spectra of these systems, like any such systems, requires cumbersome numerical calculations and can be made analytically with the help of the scattering matrix formalism, see, e.g., Ref. 11. In this work we give a simple expression determining the light wavelengths corresponding to the spectral positions of the Wood anomaly maxima depending on the parameters of the hybrid structure and apply the expression to the present experimental conditions.

II. PHENOMENOLOGICAL DESCRIPTION AND EXPERIMENT

The samples of the structures being studied are opal films (7-8 monolayers of a-SiO_2 spheres of diameter 640 nm) grown on fused silica substrates.¹²⁻¹⁴ The GST225 layers of thickness 25-150 nm were deposited on the surface of opal films in vacuum by the thermal deposition technique.⁷ The schematic picture of an opal/GST225 hybrid structure and essential geometry of the experiment are shown in Fig. 1. The light of an incandescent lamp falls on the hybrid structure at an angle θ_0 to the

normal and is detected at an angle θ (in our experiments $\theta = \theta_0$). The incidence plane (YZ) is perpendicular to the growth plane (111) of opal film.

We shall characterize a waveguide layer consisting of a top monolayer of opal film covered with GST225 film and air by an effective refractive index n_{eff} , which can be set constant in a sufficiently wide wavelength range. It is assumed that n_{eff} is the same for a direction in the plane (XY) and that perpendicular to the plane, thus being a characteristic of quasi-guided (or leaky) mode.¹¹ The value of n_{eff} depends on the direction given by horizontal projection ($\mathbf{k}_{||}$) of the wave vector (\mathbf{k}) of the wave outgoing from the structure with respect to the crystallographic direction Γ -M (or Γ -K), with the azimuthal angle between the directions given by β (see Fig.1).

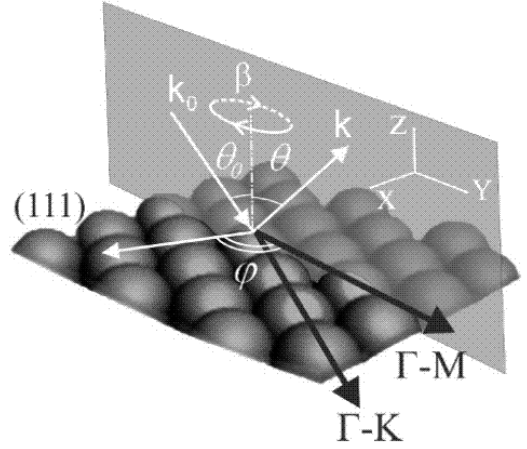


FIG. 1. Schematic image of the surface of an opal/GST225 hybrid structure and geometry of the experiment. Here are shown the incident and outgoing wave vectors \mathbf{k}_0 , \mathbf{k} and angles, θ_0 , θ , azimuthal angle β and the main crystallographic directions Γ -M and Γ -K. The angle φ is that between the direction Γ -M (or Γ -K) and some reciprocal lattice vector \mathbf{G} (white arrow in XY-plane).

Based on the usual diffraction condition (the Laue condition) the wave vectors of the propagating waves can be written as $\mathbf{k}' = \mathbf{k} + \mathbf{G}$. Here $\mathbf{G} = m_1\mathbf{b}_1 + m_2\mathbf{b}_2$ (m_1, m_2

are integers) are 2D reciprocal lattice vectors, where \mathbf{b}_1 and \mathbf{b}_2 are the elementary vectors (for hexagonal lattice $|\mathbf{b}_1| = |\mathbf{b}_2| = 4\pi/\sqrt{3}d$). We proceed under the assumption that $k' = |\mathbf{k}'| = \omega n_{eff}/c$ and the wave vector \mathbf{k} of the scattered wave is a sum $\mathbf{k} = \mathbf{k}_{\parallel} + \mathbf{k}_z$, where \mathbf{k}_z is the wave vector \mathbf{k} projection in the perpendicular direction to the waveguide layer. Due to the anisotropy of the system, both values k_z and n_{eff} depend on β and \mathbf{G} . The

concept of the effective refractive index for description of optical spectra of similar systems was earlier used in Ref. 1, but in that study the parameter k_z was ignored. Since k_z is of the same order of magnitude as \mathbf{k} and \mathbf{G} , it should be taken into account. Because of the conservation of the horizontal component \mathbf{k}_{\parallel} we take $k_{\parallel} = k \sin \theta$ and after simple mathematical transformations come to the following expression for the spectral position of the Wood anomaly peak, λ_{WP}

$$\lambda_{WP} = \frac{2\pi}{G} \frac{\sqrt{(\sin \theta \cos \varphi)^2 + (n_{eff}^2 - \sin^2 \theta)(1 + a)} - \sin \theta \cos \varphi}{1 + a} \quad (1)$$

Here φ is an angle measured from Γ -M direction in the XY plane (see Fig. 1), which defines any possible direction of vector \mathbf{G} , and $a = (k_z/G)^2$. Formally, there exists the second root of the quadratic equation for λ_{WP} (the negative sign before square root), however, from a physical sense since inequality $n > \sin \theta$ is always satisfied this solution gives negative values for λ_{WP} and therefore should be omitted. Eq. (1) can be used explicitly if the light scattering mainly occurs with a single scattering vector \mathbf{G} . This would be especially well realized for some systems with a periodic optical dielectric constant modulation in one dimension. Nevertheless, we can also use the above analytical expression for the systems with 2D dielectric constant modulation like those considered here because in case of p-polarization realized in the present experiments the electric field distribution in the waveguide layer with a change of angle θ mostly depends on the vectors \mathbf{G} corresponding to Γ -M direction. It follows from Eq. (1) that the diffraction anomalies can be formed only at wavelengths less than the value given by $\lambda_{WPM} = 2\pi(1 + n_m)/G_0$, where G_0 is the minimum magnitude of the vector \mathbf{G} and n_m is the maximum refractive index in the system.

Experimental reflection spectra from the opal/GST225 hybrid structure with GST225-film of 150 nm thickness are shown in Fig. 2 for different angles $\theta = \theta_0$ (at $\beta = 0^\circ$). In the spectra measured at an angle of $\theta_0 = 11^\circ$ one can distinguish three particular features: i) typical wavelength area of Bragg reflection in the range 1300-1350 nm, which appears due to the light diffraction from the 3D system of planes (111) of the opal film and shifts to shorter wavelengths when increasing the incidence angle of light according to the Bragg formula ($\lambda_{BP} = 2d_{111}\sqrt{\langle \varepsilon \rangle - \sin^2 \theta_0}$, where λ_{BP} is the spectral position of 3D Bragg reflection peak, d_{111} is the period of opal structure in [111] direction, $\langle \varepsilon \rangle$ is the average value of the dielectric constant of opal film); ii) wide bands in the ranges 1400-1600 nm (I_1) and 1200-1400 nm (I_2), with reflection maxima shifting to longer wavelengths (I_1) or staying almost unmoved (I_2) with increasing the angle

of light incidence (see Fig. 2b); iii) some weak intensity peaks initiated by the Fabry-Perot interference over the whole thickness of the hybrid structure. In the present study we focus on case (ii).

Figure 3 depicts the spectral positions (black squares) of the Wood anomaly maxima λ_{WP} depending on the light incidence angle for opal/GST225 hybrid structures with different thickness (h) of GST225 layer. The val-

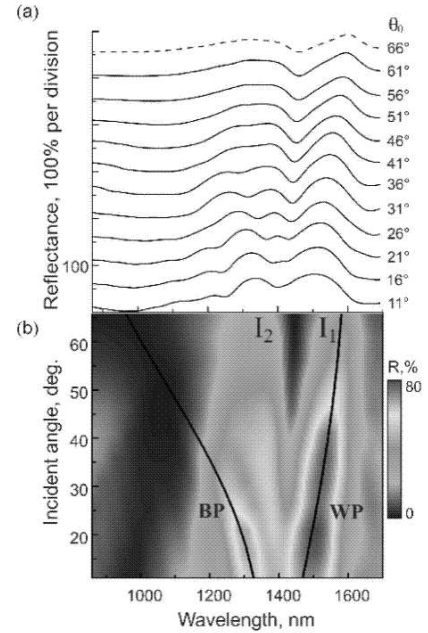


FIG. 2. (a) Experimental reflection spectra of an opal/GST225 hybrid structure for different incident angles θ_0 at $\beta = 0$. The film thickness is about 150 nm. The spectra are shifted vertically for clarity. (b) The color map is shown for improving visualization of the spectra. The solid lines passing through the spectral maxima are guides for eye and correspond to the standard Bragg diffraction (BP) from 3D opal structure and to the Wood anomalies (WP).

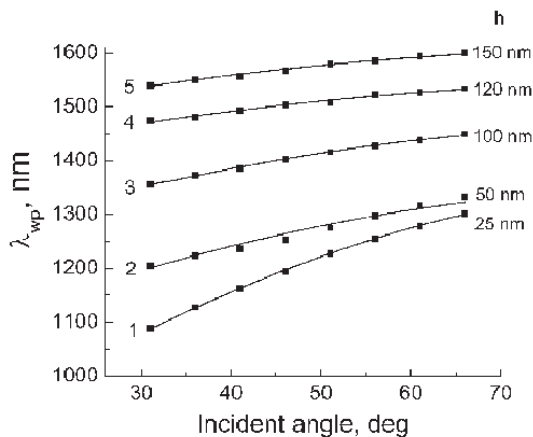


FIG. 3. Experimental values (black squares) with corresponding numerical fits (solid lines) made by Eq. (1) for wavelengths λ_{WP} for five hybrid structures differing only by the thickness (h) of the GST225 film. The corresponding parameters h , n_{eff} and a are as follows: curve 1 ($h=25$ nm, $n=1.63$, $a=0.12$); curve 2 ($h=50$ nm, $n=2.31$, $a=0.56$); curve 3 ($h=100$ nm, $n=3.08$, $a=0.97$); curve 4 ($h=120$ nm, $n=4.19$, $a=1.87$); curve 5 ($h=150$ nm, $n=4.4$, $a=1.9$); $\varphi = 180^\circ$ for all curves.

ues of h were determined from the SEM micrograph of the opal/GST225 structure cleavages. It can be seen from the figure that when thickening the film the lines $\lambda_{WP}(\theta_0)$ move to the long-wavelength region and dependence $\lambda_{WP}(\theta_0)$ is being weakened (which is related to a decrease in the derivative $\partial\lambda_{WP}/\partial\theta > 0$); it will be explained in the next section.

Experimental reflection spectra for different azimuthal angles β at the outgoing angle θ taken equal to the incidence angle $\theta_0 = 30^\circ$ are shown in Fig. 4. Since the

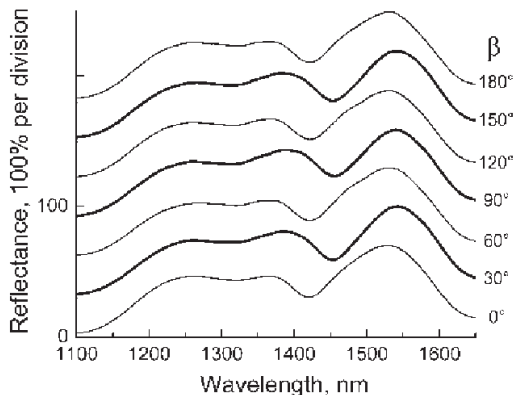


FIG. 4. Experimental reflection spectra for the opal/GST225 hybrid structure with GST225 film of the thickness 150 nm for different azimuthal angles β at an angle $\theta_0 = 30^\circ$. The spectra are shifted vertically for clarity.

system under consideration has symmetry group C_{6v} , under rotation of the incidence plane at the angle $\beta = 60^\circ$ (angle between the axes of symmetry) the spectra must be repeated, which is indeed seen from Fig. 4. Due to the symmetry, for a fixed value of the angle θ the dependence $\lambda_{WP}(\beta)$ should reach extreme values (alternating minima and maxima) at values of β equal to the multiples of 30° that also may be seen from the figure. In the vicinity of 1530 nm the shift of the spectrum reaches about 15 nm when β is varying from 0 to 30° , a reason for it will be discussed later.

III. DISCUSSION OF RESULTS

We use Eq. (1) to describe the dependence $\lambda_{WP}(\theta = \theta_0)$. The approximate values of $n_{eff} \lesssim n_{GST225}$, where n_{GST225} is the refractive index of GST225, and the wavelengths about $1\mu\text{m}$ correspond to the vectors \mathbf{G} of magnitude $|\mathbf{G}| = G_0 = 4\pi/\sqrt{3}d$, where d (≈ 640 nm) is the period of the hexagonally-ordered surface-relief grating of the hybrid structure. For the case of the scattering at angle $\varphi = 180^\circ$ experimental data points in Fig. 2(b) lie well on the curves (solid lines in Fig. 3) described by Eq. (1) under constant parameters n_{eff} and k_z , whose values are indicated in the caption of the figure. The increase in n_{eff} with chalcogenide film thickness can be explained by the fact that at the same time the average dielectric constant calculated in the effective medium approximation increases as well. Constant values of k_z for every structure for different angles θ correspond to the situations where the quasi-guided modes are formed. As is known, the usual guided modes in a three-layer planar dielectric waveguide are also characterized by special values of k_z . But compared to this case where the total internal reflection condition is always satisfied and the phase shift due to k_z -projection is a multiple of 2π ,¹⁵ for quasi-guided modes these conditions are not fulfilled and k_z can remain unchanged because of the periodicity of the structure and the corresponding electromagnetic field distribution (with the formation of modes with relatively high values of the quality factor). Actually, there is a dispersion of k_z in the medium, which we do not take into account here (just as the dispersion of n_{eff}). The propagation of electromagnetic radiation in the waveguide layer is accompanied by the scattering of the waves to the outside of the structure with a change in the effective wave vector. In the simplest case the horizontal projection of the wave vector of the scattered wave is different from the value $k_0 \sin \theta_0$ (where k_0 is the wave number of the light in the outside medium) by a single reciprocal lattice vector \mathbf{G} , in which case it is said that the incident radiation resonantly interacts with a quasi-guided mode. If the rescattering predominantly occurs with wave vector transfer $-\mathbf{G}$ it can lead to the formation of Wood anomalies at an outgoing angle $\theta = \theta_0$.

An analysis of Eq. (1) leads to the following answers for the cases of increasing and decreasing λ_{WP} with a

change in θ :

- a) $\partial\lambda_{WP}/\partial\theta > 0$ if simultaneously $\cos\varphi < 0$ and $n_{eff} > \sin\theta\sqrt{(\tan\varphi)^2(a+1)+a}$;
- b) $\partial\lambda_{WP}/\partial\theta < 0$ if simultaneously $\cos\varphi < 0$ and $n_{eff} < \sin\theta\sqrt{(\tan\varphi)^2(a+1)+a}$, and also if $\cos\varphi > 0$;
- c) $\partial\lambda_{WP}/\partial\theta = 0$ corresponds to $\lambda_{WP} = 2\pi n_{eff}/(G\sqrt{1+a})$ for any φ .

These results allow one to understand the specific character of the light scattering at different outgoing angles. For the Γ -M direction for all structures one can observe a monotonic increase of the wavelength λ_{WP} with increasing θ . This situation is in accordance with case (a) and corresponds advantageously to the backward scattering, with wave vector transfers \mathbf{G} for which $\cos\varphi < 0$ (for hexagonal lattice possible angles $\varphi = 0, \pm 60^\circ, \pm 120^\circ$ and 180°). Note that for arbitrary direction in the plane (XY) different from Γ -M and Γ -K directions (see Fig. 1), due to the asymmetry, Eq. (1) cannot be used because here one must take into account at least two reciprocal lattice vectors corresponding to the different values of φ . In these cases, however, due to the relatively small anisotropy in the plane (XY), one can also expect the appearance of a monotonic increasing dependence $\lambda_{WP}(\theta)$.

As it follows from the estimate $a = (k_z/G)^2 \sim (\sqrt{3}nd/2\lambda)^2 \sim 1$, with an increase in the angle θ the vector \mathbf{G} corresponding to $\varphi = 180^\circ$ plays an increasingly important role because at sufficiently large values of θ the condition in the case a) at $\varphi = 120^\circ$ ($n_{eff} > \sin\theta\sqrt{4a+3}$) may not be satisfied, while for the case $\varphi = 180^\circ$ the corresponding inequality ($n_{eff} > \sin\theta\sqrt{a}$) is weaker and consequently can be valid (at nearly the same values of n_{eff} and a). It is especially typical of very thin films such as the film of thickness 25 nm. To qualitatively understand the effect of the prevailing scattering at the angle $\theta = 180^\circ$ (or $\theta = 0$, which is not realized in our experiments) one should consider a ray diagram (see Fig. 5) representing the wave vectors \mathbf{k} , \mathbf{k}' and \mathbf{G} . With increasing θ the angle γ between the vectors \mathbf{k} and \mathbf{G} (or the angle χ between \mathbf{k}' and \mathbf{G}) with the opposite

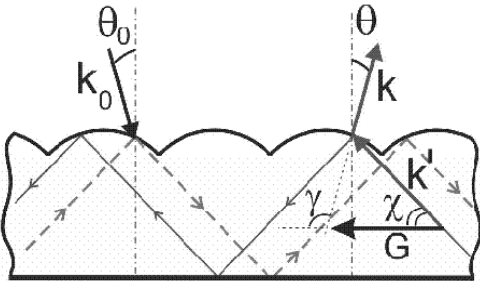


FIG. 5. The scattering geometry: light with wave vectors \mathbf{k}_0 , \mathbf{k} and \mathbf{k}' propagating in a periodic waveguide layer structure characterized by an effective refractive index. The detailed description see in the text.

direction of $\mathbf{k}_{||}$ changes noticeably more than the angles between the vector \mathbf{k} (or \mathbf{k}') and the other vectors \mathbf{G} of the same magnitude (G_0), resulting in the dependence $\lambda_{WP}(\theta)$. In other words, with an increase in angle θ the system behaves more and more asymmetrically, unlike the situation where $\theta = 0$, that is due to the scattering with wave vector transfers \mathbf{G} of magnitude $|\mathbf{G}| = G_0$. Note that the above backscattering may take place in the case of 3D opal-like photonic crystals.¹⁶

It may be noted that if the chalcogenide film thickness is not small and with its change the structure remains approximately geometrically similar to itself, then there is a quadratic dependence of the parameter a on the refractive index n_{eff} , that is $a \propto k_z^2 \propto n_{eff}^2$ (in agreement with the values presented in the caption of Fig. 3), that indirectly confirms the validity of the proposed approach with the use of the quantities n_{eff} and k_z . Another point of interest mentioned above is a flattening of the lines λ_{WP} (i.e., decrease in the derivative $\partial\lambda_{WP}/\partial\theta > 0$) while thickening the film, see Fig. 3. An analysis of Eq. (1) with $\varphi = 180^\circ$ shows that this tendency is due to the increase in the value of parameter a when increasing the film thickness h . A qualitative explanation of this effect is that the thickening of the film leads to a more uniform light scattering with wave vector transfers \mathbf{G} of magnitude $|\mathbf{G}| = G_0$ and consequently to a decrease in the derivative $\partial\lambda_{WP}/\partial\theta$.

We now address ourselves once more to Fig. 4, where the reflection spectra are presented to demonstrate small periodic changes in λ_{WP} in the vicinity of 1530 nm with a change of the azimuthal angle β . To explain it one can also exploit Eq. (1) where for the new geometry of diffraction the vectors \mathbf{G} of the magnitude equal to G_0 and making angles $\varphi = \pm 150^\circ$ with Γ -K direction should be taken into account. Since, as it directly follows from the effective medium approximation, the values of n_{eff} and $a \propto n_{eff}^2$ for the scattered light waves with $\mathbf{k}_{||}$ parallel to Γ -K direction are less than those for Γ -M direction, it can result in about the same value of λ_{WP} at a given angle θ (e.g., at $\theta_0 = 30^\circ$, see Fig. 4).

As is seen from Fig. 2, together with the long-wavelength peaks (I_1) interpreted as Wood anomalies there is a wider short-wavelength band (I_2) which can be explained as Wood anomalies corresponding to a different quasi-guided mode; in rough approximation their profiles can be described by the Lorentzian functions.¹⁷ Figure 6 shows as an example the experimental reflection spectrum of an opal/GST225 hybrid structure at an angle $\theta_0 = 66^\circ$ (see Fig. 2a) decomposed by two Lorentzians. Because of the closeness of the two peaks the Lorentz-like profiles are distorted (especially strongly between the maxima) even for large angles θ , therefore the damping rates Γ of the modes are dependent on each other. For this reason a phenomenological description of the shapes of the spectra by using the effective values n_{eff} and k_z is problematic. Another reason for this is that the value of Γ depends in a complicated manner on the outgoing angle and for its determination the exact numerical cal-

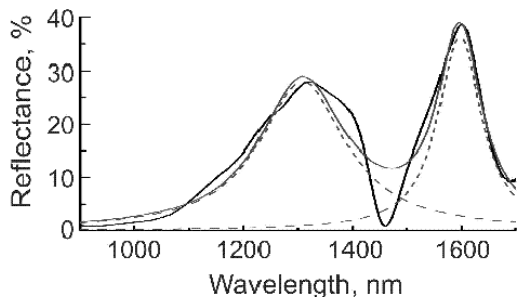


FIG. 6. Experimental reflection spectrum (black solid line) of the opal/GST225 hybrid structure (the film thickness $h = 150$ nm) at an angle $\theta_0 = 66^\circ$, and its representation by two Lorentzians (dashed lines) and by their sum (solid line).

culations are required. The wider Wood anomaly peak corresponds to a greater value of Γ and consequently to a shorter lifetime of the mode, $\tau \sim 1/\Gamma$. This mode corresponds to the situation for which $\partial\lambda_{WP}/\partial\theta \approx 0$, that is, when the light scattering with the different scattering vectors \mathbf{G} (of magnitude $|\mathbf{G}| = G_0$) occurs almost equally intensively, leading to a smaller value of τ .

IV. CONCLUSION

Wood anomalies are special types of diffraction different from Bragg one which stem from multiple wave interference and manifest themselves in optical reflection and transmission spectra.¹⁸ Depending on the geometrical form of a system, its dielectric and conductive properties and spectral characteristics of electromagnetic radiation there exist two types of Wood anomalies (Rayleigh-Wood anomaly and resonant Wood anomaly) allowing different approximate analytical description, see, e.g., Ref. 18. Diffraction anomalies of the two types, in general, can superimpose on each other as well as on specular light reflection from the film surface, 3D Bragg diffraction, Fabry-Perot oscillations and the rest of the scattered radiation. The above phenomenological description of the dependence $\lambda_{WP}(\theta)$ can also be applied to the light transmission spectra showing Wood anomalies to give the characteristic nearly linear dependence $\lambda_{WP}(\theta)$, as in the case of reflection.

In Refs. 7, 19–22 the so-called multiple Bragg diffraction in 3D photonic crystals is considered; these systems

have no additional coating serving as an optical waveguide region. The nearly linear dependence of the wavelength corresponding to a local maximum in reflectivity (or transmissivity) on the angle $\theta = \theta_0$ observed in those experiments, indicate that diffraction anomalies arising in the Bragg reflection and transmission spectra of 3D photonic crystals can be ascribed to appropriate effective quasi-guided modes (characterized by values n_{eff} and k_z). The qualitative interpretation of the multiple Bragg diffraction in 3D opal-like photonic crystals by involving the concept of Wood anomalies was proposed in Ref. 16.

It can be expected that the approach developed in the present work can also be used to estimate the locations of Wood anomalies in the reflection and transmission spectra of deterministic aperiodic structures (including quasicrystals), see, e.g., Ref. 23; in this case the vector \mathbf{G} should be replaced by appropriate diffraction vector for quasicrystal, $\mathbf{G}_{hh'}$. Despite the absence of periodicity these structures have long-range order and therefore would provide effective quasi-guided modes for propagation and scattering of light, leading to Wood anomalies in the optical spectra.²⁴

A further development of the proposed approach may be related to the study of the spectral positions of the reflection maxima and minima for waveguide grating structures characterized by a strong dispersion of the effective refractive index $n_{eff} = n_{eff}(\omega)$ of the waveguide layer (for example, due to plasmon resonance in metallic films); the corresponding spectral-angular dependencies will be obtained by solving Eq. (1) containing frequency functions $n_{eff}(\omega)$ and $a(\omega) \propto n_{eff}^2(\omega)$.

To summarize, the experimentally measured reflection spectra fall within a category of Wood anomalies because to explain them one has to consider the scattering of electromagnetic radiation expressed in terms of 2D reciprocal lattice vectors and leading to the formation of quasi-guided modes. Thus, the developed phenomenological approach allowed us to interpret the experimentally observed close to linear dependence of spectral locations of the Wood anomalies on the incident angle of light on the spatially-periodic hybrid film structure. It can be applied to other similar systems showing diffraction grating anomalies as well.

The authors wish to thank A.N. Poddubny for helpful discussions. This work was supported by the scientific program №24 of the Presidium of the Russian Academy of Sciences “Basic Foundations of the Technology of Nanostructures and Nanomaterials” and by the Linkage Grant of IB of BMBF at DLR.

* mikle.voronov@coherent.ioffe.ru

¹ L. Landström, N. Arnold, D. Brodoceanu, K. Piglmayer, and D. Bäuerle, Appl. Phys. A **83**, 271 (2006).

² K. Ishizaki and S. Noda, Nature **460**, 367 (2009).

³ I. Karakurt, C. H. Adams, P. Leiderer, J. Boneberg, and

R. F. Haglund, Opt. Lett. **35**, No. 10. (2010).

⁴ B. J. Eggleton, B. Luther-Davies, and K. Richardson, Nature Photonics **5**, 141 (2011).

⁵ S. G. Romanov, A. Regensburger, A. V. Korovin, and U. Peschel, Adv. Mater. **23**, 2515 (2011).

- ⁶ S. Raoux, W. Welnic, and D. Ielmini, *Chem. Rev.* **110**, 240 (2010).
- ⁷ S. A. Yakovlev, A. B. Pevtsov, P. V. Fomin, B. T. Melekh, E. Yu. Trofimova, D. A. Kurdyukov, and V. G. Golubev, *Techn. Phys. Lett.* **8**, 768 (2012).
- ⁸ G. W. Burr, M. J. Breitwisch, M. Franceschini, D. Garetto, K. Gopalakrishnan, B. Jackson, B. Kurdi, C. Lam, L. A. Lastras, A. Padilla B. Rajendran, S. Raoux, R. S. Shenoy, *J. Vac. Sci. Technol. B* **28**, 223 (2010).
- ⁹ M. Nardone, M. Simon, I. V. Karpov, V. G. Karpov, *J. Appl. Phys.* **112**, 071101 (2012).
- ¹⁰ A.B. Pevtsov, A.N. Poddubny, S.A. Yakovlev, D.A. Kurdyukov, and V.G. Golubev, *J. Appl. Phys.* **113**, 144311 (2013).
- ¹¹ S.G. Tikhodeev, A.L. Yablonskii, E.A. Muljarov, N.A. Gippius, and T. Ishihara, *Phys. Rev. B* **66**, 045102 (2002).
- ¹² A. B. Pevtsov, S. A. Grudinkin, A. N. Poddubny, S. F. Kaplan, D. A. Kurdyukov, and V. G. Golubev, *Semiconductors* **44**, 1537 (2010).
- ¹³ E. Y. Trofimova, A. E. Aleksenskii, S. A. Grudinkin, I. V. Korkin, D. A. Kurdyukov, and V. G. Golubev, *Colloid J.* **73**, 546 (2011).
- ¹⁴ M. V. Rybin, I. S. Sinev, A. K. Samusev, K. B. Samusev, E. Y. Trofimova, D. A. Kurdyukov, V. G. Golubev, and M. F. Limonov, *Phys. Rev. B* **87**, 125131 (2013).
- ¹⁵ A. Yariv and P. Yeh, *Optical Waves in Crystals: Propagation and Control of Laser Radiation* (Wiley, New York, 1984).
- ¹⁶ A. Tikhonov, J. Bodin, and S.A. Asher, *Phys. Rev. B* **80**, 235125 (2009).
- ¹⁷ S. Fan, J. D. Joannopoulos, *Phys. Rev. B* **65**, 235112 (2002).
- ¹⁸ A. Hessel and A.A. Oliner, *Appl. Opt.* **4**, 1275 (1965).
- ¹⁹ Henry M. van Driel and Willem L. Vos, *Phys. Rev. B* **62**, 9872 (2000).
- ²⁰ G. M. Gajiev, V. G. Golubev, D. A. Kurdyukov, A. V. Medvedev, A. B. Pevtsov, A. V. Sel'kin, and V. V. Travnikov, *Phys. Rev. B* **72**, 205115 (2005).
- ²¹ A.V. Baryshev, A.B. Khanikaev, R. Fujikawa, H. Uchida, and M. Inoue, *Phys. Rev. B* **76**, 014305 (2007).
- ²² A.V. Moroz, M.F. Limonov, M.V. Rybin, K.B. Samusev, *Physics of the Solid State*, **53** 1105 (2011).
- ²³ A.N. Poddubny, *Phys. Rev. B* **83**, 075106 (2011).
- ²⁴ The simplest system here is a 1D resonant grating waveguide structure with a rectangular profile composed of alternating segments with two different lengths to form a quasicrystal (for example, Fibonacci quasicrystal). The study of the light reflection from such a structure can be made by a method applicable to the case of the analogous periodic structure, [see D. Rosenblatt, A. Sharon, and A. A. Friesem, *IEEE J. Quantum Electron.* **33**, 2038 (1997)], that leads to a conclusion about the possibility of an appearance of Wood anomalies in the reflection spectra for some non-periodic structures having an average period (in particular, for a weakly disordered periodic structure).